School of Mathematics, Meteorology
and Physics

Department of Mathematics

Preprint MPS_2009-13

5 September 2009

On the spectra of certain Integro-Differential-Delay problems with applications in neurodynamics

by

Peter Grindrod and Dimitri Pinotsis

On the spectra of certain Integro-Di erential-Delay problems with applications in neurodynamics

Peter Grindrod and Dimitris Pinotsis

September 5, 2009

A stract

We investigate the spectrum of certain Integro-Differential-Delay equations (IDDEs) which arise naturally within spatially distributed, nonlocal, pattern formation problems. Our approach is based on the reformulation of the relevant dispersion relations with the use of the Lambert function. As a particular application of this approach, we consider the case of the Amari delay neural field equation which describes the local activity of a population of neurons taking into consideration the finite propagation speed of the electric signal. We show that if the kernel appearing in this equation is asymmetric or has a peak away from the origin, then the relevant dispersion relation yields spectra with an infinite number of branches, as opposed to finite sets of eigenvalues considered in previous works. Also, in earlier works the focus has been on the most rightward part of the spectrum and the possibility of an instability driven pattern formation. Here, we numerically survey the structure of the entire spectra and argue that a detailed knowledge of this structure is important within neurodynamical applications. Indeed, the Amari IDDE acts as a filter with the ability to recognise and respond whenever it is excited in such a way so as to resonate with one of its rightward modes, thereby amplifying such inputs and dampening others. Finally, we discuss how these results can be generalised to the case of systems of IDDEs.

*Department of Mathematics and the Centre for Integrative Neuroscience and Neurodynamics, University of Reading, UK.

such that

$$W(s)e^{W(s)} = s.$$

of the entire spectrum. This paper represents the first such survey for this dynamic Turing instability of the homogeneous steady state has been calculated and patterns emerging from this instability have been discussed in [10]. Also, the Turing instability analysis in layered 2D systems for neural fields with space-dependent delays is treated in [12]. However, it seems that the part of the spectrum corresponding to stable modes has not been studied in any full detail. In sections 3 and 4, we will show that the full spectrum of the neural field equation with delays has a rich structure previously undetected.

We consider uniform steady state solutions , $u = u_0$, where u_0 is a constant satisfying

$$u_0 = F(u_0)\varphi_0, \qquad \varphi_0 = \int_{-\infty}^{\infty} \varphi(y)dy. \tag{8}$$

Since the function $F(u)$ is uniformly bounded there will generically be an odd number of such solutions.

Now we write $u(x,t) - u_0 \propto e^{\sigma(k)t+ikx}$ in equation (7) so that, up to a linear approximation, we have

$$(\sigma(k) + 1)e^{\sigma(k)t+ikx} = F'(u_0) \int_{-\infty}^{\infty} \varphi(x-y)e^{-\sigma(k)\varepsilon|x-y|}e^{\sigma(k)t+iky}dy, \tag{9}$$

3, we focus on the case that the kernel

Then, for $\mathrm{Re}(r + \varepsilon\sigma) > 0$, equation (12) becomes

$$\sigma + 1 = \frac{e^{-\varepsilon\sigma}(1 + e^{-2r})r\,[(r + \varepsilon\sigma)\cos(2k\pi) - 2k\pi\sin(2k\pi)]}{4k^2\pi^2 + (r + \varepsilon\sigma)^2}. \qquad (18)$$

First, we consider k fixed and show that there is an infinity of values for σ corresponding to each value of k :

Multiplying both sides of equation (18) by $\varepsilon e^{\varepsilon(\sigma+1)}$, we find an equation where the dependence of the right hand side on σ is only rational, namely

$$\varepsilon(\sigma + 1)e^{\varepsilon(\sigma+1)} = \frac{\varepsilon e^{\varepsilon}(1 + e^{-2r})r\,[(r + \varepsilon\sigma)\cos(2k\pi) - 2k\pi\sin(2k\pi)]}{4k^2\pi^2 + (r + \varepsilon\sigma)^2}. \qquad (19)$$

Using the definition of the Lambert function $W(s)$ given by equation (2), we find the following expression for the spectral values

$$\sigma = \frac{1}{\varepsilon}W\,(R(k, r, \sigma)) - 1, \qquad (20)$$

where the function $R(k, r, \sigma)$ is given by the right hand side of equation (19).

Equation (20) and the fixed point theorem imply that for each branch of the Lambert function there is a corresponding value of σ. Since the Lambert function has infinitely many branches, there is an infinity of spectral values σ.

In the following, we consider some important limiting cases:

The limit $r \to \infty$

In the limit $r \to \infty$, equation (20) becomes

$$\sigma = \frac{1}{\varepsilon}W\,(\varepsilon e^{\varepsilon}\cos(2k\pi)) - 1. \qquad (21)$$

Comparing equation (21) with equation (6) we find that these two equations are the same if $\beta = 1$ and $\lambda = \cos(2k\pi)$. Therefore, for the extreme values of $\lambda = \pm 1$, ($k = 1, \pm 1, \pm 2, \ldots$ and $k = \pm\frac{1}{2}, \pm\frac{3}{2}, \ldots$), the relevant spectrum is given by the green and pink points of figure 1 (where wlog $\varepsilon = 1$).

This result should come as no surprise since as $r \to \infty$, the kernel (17) becomes a sum of two delta functions at $x = \pm 1$ representing the interaction between two "point" neurons. These coupled neurons can also be described by following system:

$$u_{1t}(t) + u_1(t) = \mu u_2(t - \varepsilon), \qquad (22)$$

$$u_{2t}(t) + u_2(t) = \mu u_1(t - \varepsilon). \tag{23}$$

Then, letting $u(t) = (u_1(t), u_2(t))(1, \pm 1)^T$, the above system reduces immediately to equation (5) with $\mu = \pm\lambda$ and spectrum depicted in figure 1.

The limit $\varepsilon \to 0$

Assuming that $\varepsilon \to 0$, namely that there is no delay, equation (18) becomes

$$\sigma + 1 = \frac{(1 + e^{-2r})\,[r^2 \cos(2k\pi) - 2rk\pi \sin(2k\pi)]}{4k^2\pi^2 + r^2}. \tag{24}$$

Figure 2. Separate spectral branches (b = 0, ±1, ±2, ±3), each starting (when k = 0) at a separate point (shown as bold) generated via the bth branch of the Lambert function, before looping through successive points. Here ε = 1 and r = 20.

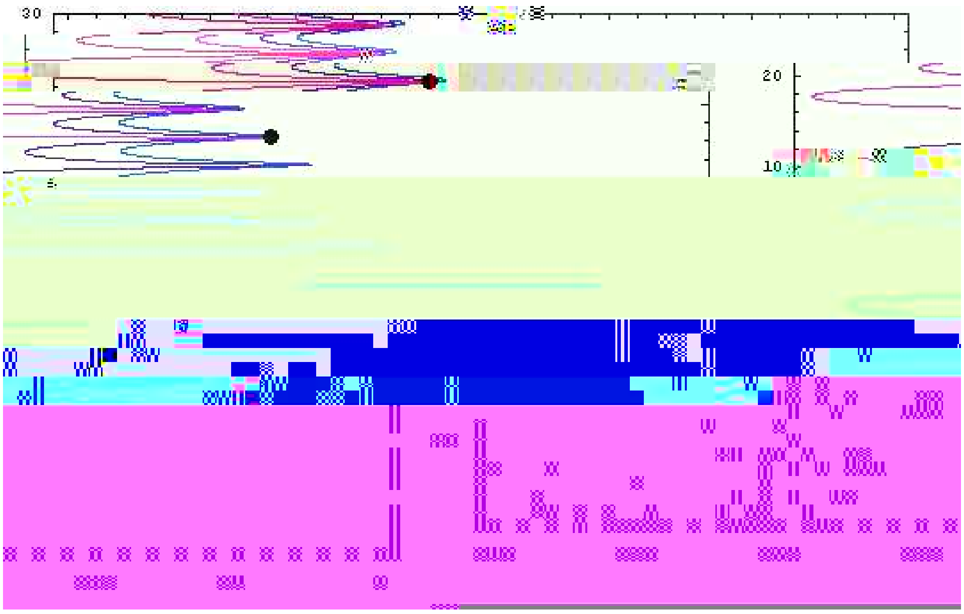

Figure 3. Sup2]TJ-361.313-14.4Td[(b)1.9477191(.26309(u)1.9482(r)(.26309(u)1.9l1.9o0.648174(

remaining real spectrum $\sigma = -1 + \hat{\varphi}(k)$. As r tends to infinity the "loops" in the spectrum become longer, with each loop approaching two parallel lines at constant imaginary values from the point at infinity, see figure 4. Finally, when ε becomes large the real part of the spectrum is lost, see figure 5.

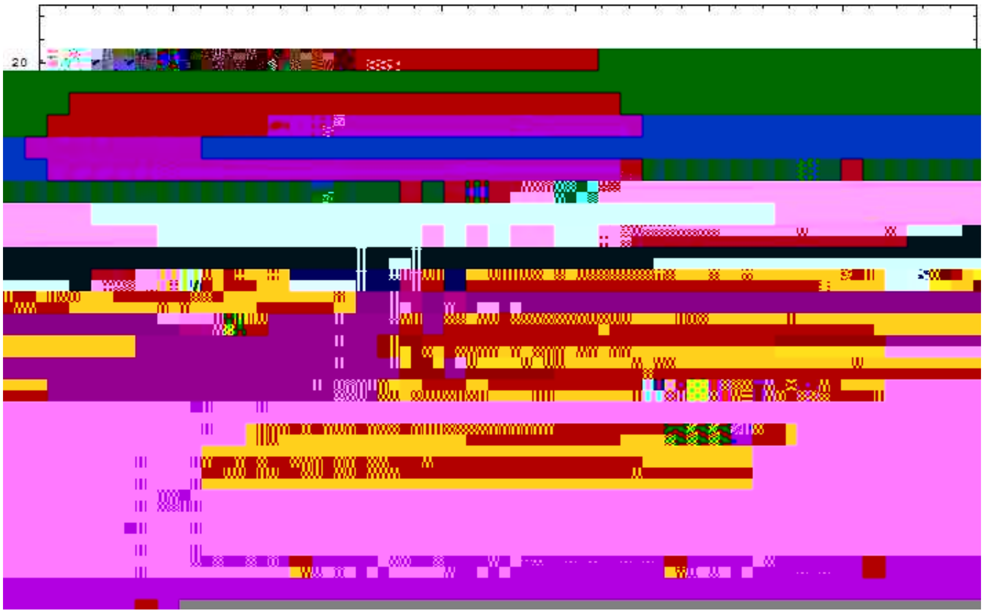

Figure 4. The spectra of the Amari equation for $\varepsilon = 1$ and $r = 200$.

Figure 5. The spectra for $\varepsilon = 20$ and $r = 2$.

Let us now show one further example. Here the kernel $\varphi(x)$ contains a sum of four terms, similar to the terms appearing in (17), each symmetric about points $x \pm 1$ and $x = \pm 2$ respectively, which we expect to resonate with constant matrix, describing the point dynamics and $\Phi(x)$ is an $m \times m$ matrix-valued smooth, integrable kernel.

We set $\Phi_0 = \int_{-\infty}^{\infty} \Phi(x)\, dx$, and assume that $u = u_0$ is a constant steady state, satifying

$$A.u_0 = \Phi_0.F(u_0).$$

Linearising about u_0, we write

$$u(x,t) - u_0 \propto e^{\sigma(k)t+ikx} v(k),$$

so that

$$(\sigma(k)I + A).v(k) = \int \Phi(x-y).dF.e^{-\sigma(k)\varepsilon|x-y|} e^{ik(y-x)}\, dy.v(k).$$

Here $dF = dF(u_0)$ is the Jacobian of F at u_0.

Define the integral operator $\hat{H}(k,\sigma(k))$ to be the (matrix-valued) Fourier transform of $\Phi(x).dF.e^{-\sigma(k)\varepsilon|x|}$. Then we have

$$(\sigma(k)I + A).v(k) = \hat{H}(k,\sigma(k)).v(k).$$

Thus the spectrum is given by

$$\det(\sigma(k)I + A - \hat{H}(k,\sigma(k))) = 0. \qquad (28)$$

Let us consider a more specific example with $m = 2$. Take

$$A = \begin{pmatrix} a_1 & 0 \\ 0 & a_2 \end{pmatrix}, \quad \Phi = \begin{pmatrix} \varphi_1(x) & 0 \\ 0 & \varphi_2(x) \end{pmatrix}, \quad dF(u_0) = \begin{pmatrix} 0 & \beta_1 \\ \beta_2 & 0 \end{pmatrix}.$$

Let

$$\hat{H}_j(k,\sigma) = \int_{-\infty}^{\infty} e^{-2\pi ikx} \varphi_j(x) e^{-\varepsilon\sigma|x|}\, dx. \qquad (29)$$

Assuming that $\hat{H}_j(k,\sigma) = e^{-\varepsilon\sigma} R_j(k,\sigma)$, where $R_j(k)$ is a polynomial in σ, The last equation yields

$$\sigma = \frac{1}{\varepsilon} W\left(\mu \sqrt{\beta_1 \beta_2}\, \varepsilon e^{\varepsilon a} (R_1 R_2)^{1/2} (k, \sigma)\right) - 1. \tag{32}$$

For example, if φ_1 and φ_2 are both given by the kernel (17), we obtain the figure below, showing the multi-branched spectrum in the case where $\mu = \pm 1$, corresponding to the purple and green curves respectively.

has a local maximum): it relatively amplifies such inputs, and dampens others (see Figure 8 below). This is “resonance” in action; the system recognises certain inputs and ignores others at no computational cost, in real time. We contend that it is these “hot spot” resonant modes that are the currency of input-output response: the latter being a dynamic and spatial distribution of neural activity. It should be emphasised that it is the delays in the Amari IDDE that produce this multiple resonance, or “harmonic” behaviour. This behaviour in turn, increases the capacity of the system to show a muliplicity of responses.

Therefore, the answer to the question raised above could be briefly stated as follows: modes of increased responsiveness of the neurodynamical system correspond to the forays of the real part of the spectrum of the Amari system.

In summary, the structure of the spectrum for the IDDE is (i) intimately connected with the choice of the kernel and (ii) a crucial component in filtering input information and producing a discrete range of resonant responses, as opposed to a passive continuum response. Of course, the nonlinearities become important away from equilibrium in the longer term. Nevertheless, for natural neurodynamical systems to perform rapid coherent signal “recognition and response” behaviour it is the complex nature of the spectra derived in this paper, even for simple systems, that is exactly what is required.

In practice, observations of neurodynamical patterns and waves via scans will allow us constrain and locate kernel behavioural properties at the meso level within the brain. Anisotropy, spatial variability, behaviour at boundaries, and piecewise continuity will make the future inverse and forward problems much harder. However, we suggest that such a programme cannot commence without a solid understanding of the rich spectral structure that is available, even for the ideal (spatially uniform, isotropic) situation considered here.

the input-output response behaviour when this system is stimulated. In practice, this may be far more important than studying the spontaneous pattern formation. Resonance (as represented by the peaks in a response surface) is a hugely efficient mechanism for tunable, responsive, learning: namely a process of producing functional quantised responses in real time relating to the form of a noisy stimulation.

The currency (or state) of such a system exists within the space of spatio-temporal patterns. This is very important in applications. If we take a single snap shot or scan - how can we judge the state of the system?

The set of possible spatio-temporal resonances is dependent on the rightward cusps of the entire spectrum, and it is large. If this is the currency of information processing within such systems (like our brains) then in this single concept, we attain both capacity and efficiency (since neural resonance requires no computation and responds in real time). This idea suggests that in seeking to understand reasoning processes from patterns and connectivities within single fMRI scans [16] we are looking in the wrong place: we must see the evolution of such activity over time as the response to the upstream stimuli.

Acknowledgement. The authors acknowledge support from EPSRC

[7] D Henry,